Multidimensional attosecond photoelectron spectroscopy with shaped pulses and quantum optical fields

Saar Rahav and Shaul Mukamel
Department of Chemistry, University of California, Irvine, California 92697, USA
(Received 26 November 2009; published 10 June 2010)

Correlation function expressions for multidimensional photoelectron signals obtained for the response of electrons and nuclei in molecules to multiple ultrafast optical or x-ray pulses are derived using a superoperator formalism. For classical fields and quantum matter, these signals are recast as modulus squares of transition amplitudes which depend on the pulse bandshapes. A vibrational wave-packet representation which does not involve amplitudes is derived when the nuclear dynamics is calculated classically. In the case of a quantum radiation field, the signals depend on multipoint correlation functions of field operators. Photoelectron spectroscopy with entangled photons may be studied using this formalism.

DOI: 10.1103/PhysRevA.81.063810 PACS number(s): 42.65.Re, 82.80.Pv

I. INTRODUCTION

Photoelectron (photon-in–electron-out) spectroscopy is a powerful tool for probing orbital energies in molecules and crystals [1,2]. The technique had been extended to the time domain over the past 15 years [3–10]. In time-resolved photoelectron spectroscopy (TRPES), the system is prepared in a nonequilibrium state by a laser pulse, undergoes time evolution for a delay time t, and is eventually probed by detecting the electrons generated by a second, ionizing, pulse. The distribution of the electron kinetic energy (ε) reveals the underlying dynamics through its parametric dependence on the time delay. The relaxation of electronic excitations in crystals such as copper [4] and graphite [5] was studied by varying the time delay between a pump pulse, which perturbs the Fermi distribution, and a probe pulse. TRPES was also used to study the vibrational dynamics of I_2^- [9] as well as conical intersections and nonadiabatic transitions in DNA bases such as uracil and thymine [7,8]. Here the pump creates a vibrational wave packet and the signal contains signatures of its evolution.

All of these applications contain a single time delay which together with the electron kinetic energy provides a two-dimensional (2D) signal. This technique can be viewed as a two-dimensional photoelectron spectroscopy (2DPES), since the signal $S(\varepsilon,t)$ depends on two parameters. Recent advances in laser extreme ultraviolet (XUV) and x-ray pulse generation [11–15] allow one to extend this technique to higher dimensions. The material system (e.g., atom, molecule, or a crystal) interacts with a sequence of short infrared, visible, XUV or x-ray pump pulses. A final ionizing pulse then generates photoelectrons which are energy resolved and detected. By displaying the signal and its variation with various time delays between the pulses we obtain n-dimensional photoelectron spectroscopy (nDPES). Two pump pulses with a delay t_1, for example, generate a three-dimensional (3D) signal $S(\varepsilon,t_1,t_2)$ where t_2 is the delay of the ionizing probe. Apart from the time delays, one can use pulse shaping to vary pulse envelopes, phases, polarizations, and carrier frequencies to provide novel information on electronic and molecular dynamics. Multidimensional spectroscopy originated in nuclear magnetic resonance (NMR) [16] and was extended to the infrared and visible [17].

In this paper we develop a formalism for computing nDPES. Multidimensional optical signals where fields are detected (e.g., wave mixing) are usually calculated in terms of nonlinear response function and susceptibilities. Photon counting measurements, on the other hand, are best described by sequences of transition amplitudes (generalized Fermi golden rule) using the celebrated formalism of Glauber [18]. The connection of the two approaches was discussed recently [19,20]. Since electron detection is more closely connected to photon counting, we recast these signals in terms of transition amplitudes, which are more intuitive and easier to calculate than susceptibilities. Signals obtained with temporally well-separated pulses and arbitrary bandshapes are calculated. The matter enters through transition amplitudes which may contain interesting interferences between pathways. The formalism can also be applied to attosecond electron dynamics where the pump ionizes the molecule to create one or several holes (core or valence type) and the subsequent hole migration [21–23] is probed by a second pulse. We further develop a classical description of the signal in terms of vibrational wave packets. Photon-in–photon-out signals are complementary to photon-in–electron-out signals [24–28]. The detection of photoelectrons is more sensitive compared to photons.

All the above applications assume that the radiation fields are classical. Quantum fields provide many additional control parameters and could open up new spectroscopic techniques. Photoelectron spectroscopy (PES) with classical fields can be expressed through causal response functions of the material system alone. To describe the coupling of two quantum systems (molecule and field), we must formulate the problem using superoperator nonequilibrium Green's functions (SNGFs) which represent the coupled response and spontaneous fluctuations of both systems [29,30]. We extend the classical field results to quantum fields and express the signals using sums of products of matter and field correlation functions. One possible future application of quantum fields is to carry out PES with entangled photons [31,32]. As experimental techniques for generating entangled fields are improved, these parameters of the photon wave function provide a new class of control knobs for multidimensional spectroscopy.

In Sec. II we derive an expression for the photoelectron signal. When the photoionizing pulse is temporally well separated from the other pulses used to prepare the system in a coherent wave packet, the signal takes a form of an absolute square of a transition amplitude. Signals resulting from several temporally separated pulses and parameterized by the delay periods are considered in Sec. III. In Sec. IV we derive a classical expression for PES for vibrational wave packets. PES signals generated by quantum laser fields are calculated in Sec. V. Finally, the photoelectron signal is compared to the absorption of the probe pulse in Sec. VI.

II. SUPEROPERATOR CORRELATION FUNCTIONS FOR PHOTOELECTRON SIGNALS; TRANSITION AMPLITUDES

In this section we use the response function formalism of nonlinear optical spectroscopy to derive compact expressions for the TREPS signals in terms of Liouville space correlation functions. We consider a molecule driven by a series of laser or x-ray pulses which may be ionizing or not. We will divide the many-body molecular states into two groups, undetected ($|\nu\rangle$) and detected ($|f\rangle$) ionized continuum states created by the last pulse. The system is described by the Hamiltonian,

$$\mathcal{H} = \mathcal{H}_0 + \mathcal{H}'(t), \tag{1}$$

$$\mathcal{H}_0 = \sum_\nu \varepsilon_\nu |\nu\rangle\langle\nu| + \varepsilon_f |f\rangle\langle f|. \tag{2}$$

For brevity, the index f also includes the internal molecular quantum numbers, as well as the photoelectron momentum. The energy of the final state is therefore the sum of the energy of the ion and the kinetic energy of the electron, $\varepsilon_f = \varepsilon_f^+ + \varepsilon_{\mathbf{k}}$. Formally, a sum over all final states should appear in Eq. (2). This sum is omitted for brevity, but the effects of many possible final states are easily taken care for by reintroducing the sum (limited to states with a given kinetic energy of the photoelectron) at the end.

The interaction with the laser pulses is

$$\mathcal{H}'(t) = -E(t)\hat{V}, \tag{3}$$

where $E(t)$ is the electric field and $\hat{V} = \sum_{\nu\nu'} \mu_{\nu\nu'} |\nu\rangle\langle\nu'|$ is the electronic dipole operator. The pump pulses (E^p) create an electronic wave packet in the molecule. This wave packet evolves freely until the interaction with the final, ionizing, detection pulse E^d, which is assumed to be temporally well separated from the pump. We write

$$E(t) = E^d(t) + E^p(t). \tag{4}$$

With the help of Eq. (4) we can also write $\mathcal{H}'(t) = \mathcal{H}^d(t) + \mathcal{H}^p(t)$.

The photoelectron signal is obtained by collecting the ejected electrons and resolving their kinetic energy $\varepsilon_{\mathbf{k}}$. In the following we focus on the time-integrated signal, given by the total number of ejected photoelectrons (with a given kinetic energy) generated by the final pulse,

$$\tilde{S}(\varepsilon) = \mathrm{Tr}\, \hat{P}^f \hat{\rho}(t), \tag{5}$$

where $\hat{\rho}(t)$ is the system density matrix at an arbitrary time after the interaction with the detection pulse. We will expand $\hat{\rho}(t)$ to second order in the interaction with the detection pulse $\mathcal{H}^d$. $\hat{P}^f \equiv |f\rangle\langle f|$ is a projection onto the final molecular state. The dependence of $\tilde{S}(\varepsilon)$ on the photoelectron kinetic energy ε follows from the the final state f, whose photon kinetic energy must satisfy $\varepsilon_{\mathbf{k}} = \varepsilon$. As stated before, when several such states exist they should be summed over.

Equation (5) states that the signal is proportional to the state f population after the detection pulse. Note that this description pertains for a finite pulse measurement; otherwise, it is not possible to define times later than the last interaction. The signal does not depend on t, since there is no field after the last pulse and no transitions are possible. This approach is not suitable for frequency-domain measurements, and the signal should instead be defined as the steady-state rate of transitions to the final state.

The density matrix $\hat{\rho}(t)$, which is driven out of its initial value $\hat{\rho}_0$ by interactions with the pump pulses, will be calculated perturbatively. To that end, we introduce superoperator notation: with each ordinary operator $\hat{A}$ in Hilbert space we associate a left (L) and a right (R) superoperator defined by its action on another operator $\hat{X}$,

$$\hat{A}_L \hat{X} \equiv \hat{A}\hat{X} \tag{6}$$

$$\hat{A}_R \hat{X} \equiv \hat{X}\hat{A}. \tag{7}$$

Interaction-picture superoperators are given by

$$\hat{A}_\nu(t) \equiv (e^{\frac{i}{\hbar}\mathcal{H}_0 t} \hat{A} e^{-\frac{i}{\hbar}\mathcal{H}_0 t})_\nu, \quad \nu = L, R. \tag{8}$$

We further define the following two linear combinations of the left and right superoperators,

$$\hat{A}_\pm \equiv \frac{1}{\sqrt{2}}(\hat{A}_L \pm \hat{A}_R). \tag{9}$$

In the interaction picture, the photoelectron signal can be written as [29,33]

$$\tilde{S}(\varepsilon) = \left\langle \mathcal{T} \hat{P}_L^f(t) \exp_+ \left[-\frac{i}{\hbar} \int_{-\infty}^{t} d\tau \sqrt{2} \mathcal{H}'_-(\tau) \right] \right\rangle_0, \tag{10}$$

where the time-ordering operator $\mathcal{T}$, when acting on a product of superoperators, rearranges them so that their time arguments increase from right to left. $\langle \cdots \rangle_0$ denotes an average over the initial ground-state density matrix, $\hat{\rho}_0 = |g\rangle\langle g|$. All quantities in Eq. (10) are interaction picture superoperators [see Eq. (8)].

In Hilbert space, Eq. (10) takes the form,

$$\tilde{S}(\varepsilon) = \mathrm{Tr} \exp_- \left[\frac{i}{\hbar} \int_{-\infty}^{t} d\tau \mathcal{H}'(\tau) \right] |f(t)\rangle\langle f(t)| \times \exp_+ \left[-\frac{i}{\hbar} \int_{-\infty}^{t} d\tau \mathcal{H}'(\tau) \right] \hat{\rho}_0(t_0). \tag{11}$$

For classical optical fields $\tilde{S}$ breaks into a sum of products of transition amplitudes. The extension to quantum fields is given in Sec. V. With $\hat{\rho}_0 = \hat{\rho}_{\mathrm{field}} \otimes \hat{\rho}_{\mathrm{matter}}$, the material part still factorize into a product of two amplitudes, but they are multiplied by a field correlation function which is not generally factorizable.

The roles of the detection and pump pulses can be separated by expanding the ordered exponentials, and identifying the last interaction (in each amplitude) with the detection pulse, and all previous ones with the pump pulses. Since there are no

interactions following the detection pulse, the upper limit of the time integrations can be extended to infinity. This gives the signal to second order in its interaction with the detection pulse,

$$\tilde{S}(\varepsilon) = \frac{1}{\hbar^2}\int d\tau_1 d\tau_2 e^{i\omega_{fg}(\tau_1-\tau_2)} T_{fg}(\tau_1) T^{\dagger}_{gf}(\tau_2), \qquad (12)$$

where we have defined the *transition amplitudes* between states g and f,

$$T_{fg}(t) \equiv \langle f(t)|\mathcal{H}^d(t)\exp_+\left[-\frac{i}{\hbar}\int_{-\infty}^{t} d\tau' \mathcal{H}^p(\tau')\right]|g(t_0)\rangle \times e^{i\varepsilon_g(t-t_0)/\hbar}, \qquad (13)$$

and, similarly,

$$T^{\dagger}_{gf}(t) = \langle g(t_0)|\exp_-\left[\frac{i}{\hbar}\int_{-\infty}^{t} d\tau' \mathcal{H}^p(\tau')\right]\mathcal{H}^d(t)|f(t)\rangle \times e^{-i\varepsilon_g(t-t_0)/\hbar}. \qquad (14)$$

The last phase factor was added to ensure that in the absence of the pump we get $T_{fg}(t) = -V_{fg}E^{(d)}(t)$. In writing Eq. (13) we have made a common approximation in PES, namely that the dipole operator matrix element depends only weakly on the momentum of the scattering electron.

The signal Eq. (12) contains all orders in the interactions $\mathcal{H}^p$ with the pump pulses. It represents the signal as a correlation function of $\mathcal{H}^d$ interactions averaged over the density matrix which evolves under the influence of the other pulses. This is depicted as the loop diagram, shown in Fig. 1.

We now define the frequency domain transition amplitudes:

$$T_{\nu\nu'}(\omega) = \int dt T_{\nu\nu'}(t) e^{i\omega t}, \qquad (15)$$

$$T_{\nu\nu'}(t) = \frac{1}{2\pi}\int d\omega T_{\nu\nu'}(\omega) e^{-i\omega t}. \qquad (16)$$

Combining Eq. (12) with Eqs. (15) and (16), we can recast the signal in the frequency domain:

$$\tilde{S}(\varepsilon) = \hbar^{-2}\int d\omega |T_{fg}(\omega)|^2 \rho_f(\varepsilon)\delta(\omega-\omega_{fg}) = \hbar^{-2}|T_{fg}(\omega_{fg})|^2\rho_f(\varepsilon). \qquad (17)$$

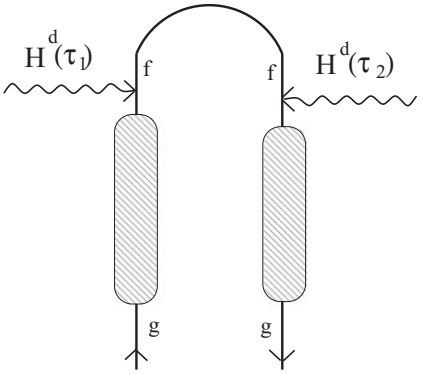

FIG. 1. Schematic depiction of a photoelectron signal, given by Eq. (12). The shaded area in the left (right) branch of the loop represents T_{fg} ($T^{\dagger}_{gf}$). The signal depends parametrically on the time delays between the various pulses.

The photoelectron signal is given by a modulus square of a transition amplitude, evaluated at the transition frequency, and multiplied by the density of scattering states, $\rho_f(\varepsilon)$. (The density of states results from summation over final states with the same photoelectron kinetic energy which was omitted until this point.) It should be noted that both factors depend on the electron kinetic energy through $\varepsilon^+_f + \varepsilon - \varepsilon_g = \hbar\omega_{fg}$, where ε^+_f is the internal energy of the ion. Equation (17) should be averaged over the initial-state distribution and summed over the possible ionic final states. Adding pulse polarizations and including angular averaging in randomly oriented samples is straightforward and may reveal interesting details, but goes beyond the scope of this paper.

The transition amplitudes in Eq. (17) can be expanded in powers of the various pulses,

$$T_{fg}(\omega) = \int d\omega_1 E^d(\omega_1)\tilde{T}^{(1)}_{fg}(\omega_1)\delta(\omega-\omega_1) + (2\pi\hbar)^{-1}\int d\omega_1 d\omega_2 E^p(\omega_1)E^d(\omega_2)\tilde{T}^{(2)}_{fg}(\omega_2,\omega_1) \times \delta(\omega-\omega_1-\omega_2) + (2\pi\hbar)^{-2}\int d\omega_1 d\omega_2 d\omega_3 E^p(\omega_1)E^p(\omega_2)E^d(\omega_3) \times \tilde{T}^{(3)}_{fg}(\omega_3,\omega_2,\omega_1)\delta(\omega-\omega_1-\omega_2-\omega_3)+\cdots, \qquad (18)$$

where $\tilde{T}$ denote bare transition amplitudes of the same $g \to f$ molecular transition. Equation (17) shows interference between contributions of different orders in the field or different combinations of field modes, provided that the fields are phase coherent. Such interference between one- and two-photon absorption was first pointed out by Glauber [18] and can be used to control the nonlinear optical properties of materials [34].

To proceed further one must specify the form of the interactions with the pump pulses. This will be done in the next section.

III. PHOTOELECTRON SIGNALS INDUCED BY TEMPORALLY WELL-SEPARATED PULSES

In the following we calculate the photoelectron signal induced by a series of pump pulses with variable delays, followed by a final ionizing detection pulse. The pulse configuration is depicted in Fig. 2. The interaction with the pump is dominated by second-order contributions in the field, with $E^{(1)}(t) \equiv E^p(t)$ centered at time τ_1 and $E^{(2)}(t) \equiv E^d(t)$ centered at time τ_2.

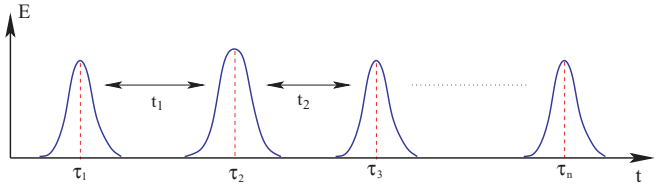

FIG. 2. (Color online) The pump-probe pulse configuration. The system interacts with several well-separated pulses, centered at times τ_i. The time delays between the pulses are $t_i = \tau_{i+1} - \tau_i$.

Equation (17) expresses the signal as the absolute square of a transition amplitude in Hilbert space. For temporally well-separated pulses we can calculate all the time integrals explicitly and obtain compact frequency-domain expressions [35] which reveal the roles of the time delays and the bandshapes. We introduce the modified Fourier transform:

$$\tilde{E}^{(j)}(\omega)e^{i\omega\tau_j} \equiv \int dt\, E^{(j)}(t)e^{i\omega t} \tag{19}$$

$$E^{(j)}(t) = \frac{1}{2\pi}\int d\omega \tilde{E}^{(j)}(\omega)e^{i\omega\tau_j - i\omega t}. \tag{20}$$

The jth pulse is centered at τ_j. $\tilde{E}(\omega)$ represents a pulse centered at $\tau = 0$ (Fig. 2).

For ordinary PES where there is no pump, and we take Eq. (13) to first order,

$$T_{fg}^{(1)}(t) = -V_{fg}E^{(1)}(t). \tag{21}$$

[Here, $E^{(1)}$ is the final ionizing pulse—the only pulse in this case]. The Fourier transform of Eq. (21) gives

$$T_{fg}^{(1)}(\omega_{fg}) = -V_{fg}\tilde{E}^{(1)}(\omega_{fg})e^{i\omega_{fg}\tau_1}, \tag{22}$$

resulting in the common Fermi golden rule expression of PES:

$$\tilde{S}^{(2)}(\varepsilon) = \hbar^{-2}\rho_f(\varepsilon)|V_{fg}|^2|\tilde{E}(\omega_{fg})|^2. \tag{23}$$

We next calculate the pump-probe signal with a single pump pulse by expanding the time-ordered exponent in Eq. (13) to first order,

$$T_{fg}^{(2)}(t) = -\frac{i}{\hbar}\int_{t_0}^{t} d\tau\, E^{(2)}(t) \times E^{(1)}(\tau)\langle f|\hat{V}\hat{G}(t,\tau)\hat{V}\hat{G}(\tau,t_0)|g\rangle e^{i\varepsilon_g(t-t_0)/\hbar}, \tag{24}$$

where $\hat{G}(t,t') \equiv \theta(t-t')e^{-\frac{i}{\hbar}\mathcal{H}_0(t-t')}$. For well-separated pulses, one can extend the upper limit of integration over τ to infinity [35] since the only times t that contribute are well beyond the nonvanishing region of $E^{(1)}(\tau)$. Expanding in eigenstates of $\mathcal{H}_0$, and performing the τ integration, we find

$$T_{fg}^{(2)}(t;t_1) = -\frac{i}{\hbar}\sum_{v} V_{fv}V_{vg}E^{(2)}(t)\tilde{E}^{(1)}(\omega_{vg})e^{-i\omega_{vg}\tau_1}e^{-i\omega_{vg}t}, \tag{25}$$

or in the frequency domain,

$$T_{fg}^{(2)}(\omega_{fg};t_1) = -\frac{i}{\hbar}e^{i\omega_{fg}\tau_2}\sum_{v} V_{fv}V_{vg}\tilde{E}^{(2)}(\omega_{fv})\tilde{E}^{(1)}(\omega_{vg})e^{-i\omega_{vg}t_1}. \tag{26}$$

The parametric dependence on the delay t_1, originating from the fact that the pulses are centered around times τ_1, τ_2, is now explicitly seen. The corresponding 2D signal is given by

$$\tilde{S}^{(4)}(\varepsilon,t_1) = \hbar^{-2}\left|T_{fg}^{(2)}(\omega_{fg};t_1)\right|^2\rho_f(\varepsilon), \tag{27}$$

with $\varepsilon = \hbar\omega_{fv} + \hbar\omega_{vg} - \varepsilon_f^+$. It is not hard to generalize this calculation to any number of temporally well-separated pump pulses. For a process with n pulses we denote $E^p(t) = \sum_{i=1}^{n-1} E^{(i)}(t)$ and $E^d(t) = E^{(n)}(t)$, where $E^{(i)}(t)$ is the field of the ith pulse, centered at time τ_i. The resulting signal is n dimensional, since it depends on $n-1$ delay times $t_j \equiv \tau_{j+1} - \tau_j$ and the photoelectron kinetic energy.

We assume that the molecule interacts with each pulse once. The signal is obtained by expanding the time-ordered exponent of Eq. (13). The next order is given by

$$T_{fg}^{(3)}(\omega_{fg};t_2,t_1) = \hbar^{-2}e^{i\omega_{fg}\tau_3}\sum_{v_1,v_2} e^{-i\omega_{v_2g}t_2}e^{-i\omega_{v_1g}t_1}V_{fv_2}V_{v_2v_1}V_{v_1g} \times \tilde{E}^{(3)}(\omega_{fv_2})\tilde{E}^{(2)}(\omega_{v_2v_1})\tilde{E}^{(1)}(\omega_{v_1g}), \tag{28}$$

resulting in the 3D signal,

$$\tilde{S}^{(6)}(\varepsilon,t_2,t_1) = \hbar^{-2}\left|T_{fg}^{(3)}(\omega_{fg};t_2,t_1)\right|^2\rho_f(\varepsilon), \tag{29}$$

with $\varepsilon = \hbar\omega_{fv_2} + \hbar\omega_{v_2v_1} + \hbar\omega_{v_1g} - \varepsilon_f^+$. The generalization to high orders is straightforward.

Typically, the photoelectron signal varies slowly with energy ε, except around the thresholds of new scattering f states. To better reveal the transitions as peaks, rather then step functions, PES signals are usually displayed as the derivative of $\tilde{S}$ with respect to an energy variable (i.e., the kinetic energy of the photoelectrons or the carrier frequency of one of the pulses). In frequency domain experiments one varies the laser frequency to resolve different thresholds. The bandwidths $\tilde{E}^{(j)}(\omega)$ select the relevant transitions.

The signals calculated above contain only some contribution out of a host of possible processes described by Eq. (17). Interferences among various contributions may be important. As an example, let us consider a three-pulse process, with two pump pulses and one ionizing pulse. Equation (28) is indeed the leading order contribution which interacts with all the pulses. However, the transition matrix element in Eq. (13) may include many other processes, some of which are lower order in the field. When the transition amplitude is squared, one finds interferences between various processes. For instance, the interference between (28) and a lower-order process which only interacts with one or two of the pulses will still depend on all the time delays.

IV. SEMICLASSICAL WAVE-PACKET CALCULATION OF THE PHOTOELECTRON SIGNAL

A laser pulse interacting with a molecule creates a wave packet composed of a coherent superposition of many vibrational levels whose exact description is rather complicated. Instead, one may approximate the wave-packet vibrational dynamics as classical, while keeping the quantum nature of the electronic excitations [36]. In this case the signal may no longer be described by amplitudes. This type of approximation has been widely used since the 1980s and is presented in Ref. [37] and in Chapter 7 of Ref. [38].

We consider a molecule with three manifolds of vibronic states. The ground state, g, an excited state, e, and a family of scattering states, described by the many-body state of the ionized molecule f, and the momentum of the ejected electron $\mathbf{k}$. The free molecule is represented by the Hamiltonian:

$$\mathcal{H}_0 = \sum_{a=g,e,f\mathbf{k}} |a\rangle\mathcal{H}_a(\hat{\mathbf{q}})\langle a|. \tag{30}$$

$\mathcal{H}_a(\hat{\mathbf{q}})$ is an operator in the nuclear Hilbert space. It is given by

$$\mathcal{H}_a(\hat{\mathbf{q}}) = \varepsilon_a + T(\hat{\mathbf{q}}) + W_a(\hat{\mathbf{q}}), \tag{31}$$

where T is the kinetic energy and W_a the potential energy. ε_a is the electronic energy, which is chosen so that all the manifold ground states of $T + W_a$ will have the same energy. The dipole coupling between the system and the laser pulses is also an operator in the nuclear coordinates:

$$\hat{V} = \sum_{\substack{a,a'=g,e,f\mathbf{k} \\ a\neq a'}} V_{aa'}(\hat{\mathbf{q}})|a\rangle\langle a'|. \tag{32}$$

To approximate the nuclear dynamics as classical, we replace the dynamics of both ket and bra by classical phase space equations of motion. As a result the approach used in Sec. II, where the dynamics ket and bra were calculated separately, is not applicable.

We concentrate on the simplest pump-probe process, with a single pump pulse. Starting from Eq. (12) we expand the time-ordered exponent to second order and select the terms with one interaction from the left and one from the right, neglecting pump-induced Raman processes. There are two such contributions depending on the time ordering of the pump left and right interactions. These are then combined to give

$$\tilde{S}^{pp}(\varepsilon) = -\frac{2}{\hbar^4}\sum_{\varepsilon_{\mathbf{k}}=\varepsilon} \mathrm{Tr}_N \mathrm{Im}\Bigg\{ i^3 \int dt \int_{t_0}^{t} d\tau_3' \int_{t_0}^{\tau_3'} d\tau_2' d\tau_1' E^{(2)}(t)E^{(2)}(\tau_3')E^{(1)}(\tau_2')E^{(1)}(\tau_1') \times V_{f,e}(\hat{\mathbf{q}}) e^{-\frac{i}{\hbar}\mathcal{H}_e(\hat{\mathbf{q}})(t-\tau_2')} V_{e,g}(\hat{\mathbf{q}}) e^{-\frac{i}{\hbar}\mathcal{H}_g(\hat{\mathbf{q}})(\tau_2'-t_0)} \rho_g(\hat{\mathbf{q}}) e^{\frac{i}{\hbar}\mathcal{H}_g(\hat{\mathbf{q}})(\tau_1'-t_0)} V_{e,g}^{\dagger}(\hat{\mathbf{q}}) e^{\frac{i}{\hbar}\mathcal{H}_e(\hat{\mathbf{q}})(\tau_3'-\tau_1')} V_{f,e}^{\dagger}(\hat{\mathbf{q}}) e^{\frac{i}{\hbar}\mathcal{H}_{f\mathbf{k}}(\hat{\mathbf{q}})(t-\tau_3')} \Bigg\}, \tag{33}$$

where we assumed that the dipole interaction does not depend on $\mathbf{k}$. Tr_N denotes the trace over the nuclear subspace, while $\rho_g(\hat{\mathbf{q}})$ is the ground-state density matrix,

$$\rho_g(\hat{\mathbf{q}}) = \frac{e^{-\beta\mathcal{H}_g(\hat{\mathbf{q}})}}{\mathrm{Tr}_N e^{-\beta\mathcal{H}_g(\hat{\mathbf{q}})}}. \tag{34}$$

The nuclear dynamics will be approximated by a combination of classical dynamics and additional phases. We first choose a suitable reference Hamiltonian,

$$\mathcal{H}_{\mathrm{ref}}(\hat{\mathbf{q}},t) = \begin{cases} \mathcal{H}_g(\hat{\mathbf{q}}) & t \leqslant \tau_1 \\ \mathcal{H}_e(\hat{\mathbf{q}}) & \tau_1 \leqslant t < \tau_2 \\ \mathcal{H}_{f\mathbf{k}}(\hat{\mathbf{q}}) & \tau_2 \leqslant t. \end{cases} \tag{35}$$

The elements in Eq. (33), which are operators in the nuclear Hilbert space, may then be recast into the interaction picture with respect to the reference Hamiltonian. For example,

$$\theta(t_2-t_1)e^{-\frac{i}{\hbar}\mathcal{H}_a(t_2-t_1)} = \theta(t_2-t_1)\exp_+\left[-\frac{i}{\hbar}\int_{t_1}^{t_2} d\tau \mathcal{H}_{\mathrm{ref}}(\tau)\right] \times \exp_+\left[-\frac{i}{\hbar}\int_{t_1}^{t_2} d\tau \overline{W}_a(\tau)\right], \tag{36}$$

where

$$\overline{W}_a(\tau) = \exp_-\left[\frac{i}{\hbar}\int_{t_1}^{\tau} d\tau \mathcal{H}_{\mathrm{ref}}(\tau)\right][\mathcal{H}_a - \mathcal{H}_{\mathrm{ref}}(\tau)] \times \exp_+\left[-\frac{i}{\hbar}\int_{t_1}^{\tau} d\tau \mathcal{H}_{ref}(\tau)\right]. \tag{37}$$

This semiclassical approximation consists of replacing the evolution of both the ket and the bra by classical evolution with respect to $\mathcal{H}_{\mathrm{ref}}$. The dynamics is given by a collection of classical phase-space trajectories $\Gamma_t \equiv [\mathbf{q}(t),\mathbf{p}(t)]$ of the reference Hamiltonian:

$$\dot{q}_i = \frac{\partial}{\partial p_i}\mathcal{H}_{\mathrm{ref}}(\Gamma) \tag{38}$$

$$\dot{p}_i = -\frac{\partial}{\partial q_i}\mathcal{H}_{\mathrm{ref}}(\Gamma). \tag{39}$$

All other functions of $\hat{\mathbf{q}}$, such as $\overline{W}_a$ or V, are replaced by their value at the corresponding classical phase-space point along the trajectory. The initial conditions are distributed according to the classical analog of ρ_g,

$$P_g(\Gamma_{t_0}) = \frac{e^{-\beta\mathcal{H}_{\mathrm{ref}}(\Gamma_{t_0})}}{\int d\Gamma_{t_0} e^{-\beta\mathcal{H}_{\mathrm{ref}}(\Gamma_{t_0})}}. \tag{40}$$

The time-integrated signal is finally given by

$$\tilde{S}_{sc}^{pp}(\varepsilon,t_1) = -\frac{2}{\hbar^4}\sum_{\varepsilon_{\mathbf{k}}=\varepsilon}\int d\Gamma_{t_0}\int dt\int_{t_0}^{t} d\tau_3'\int_{t_0}^{\tau_3'} d\tau_2' d\tau_1' \mathrm{Im}\Big\{ i^3 E^{(2)}(t)E^{(2)}(\tau_3')E^{(1)}(\tau_2')E^{(1)}(\tau_1')V_{f,e}(\mathbf{q}(t))V_{e,g}(\mathbf{q}(\tau_2'))V_{f,e}^{*}(\mathbf{q}(\tau_3'))V_{e,g}^{*}(\mathbf{q}(\tau_1')) \times e^{-\frac{i}{\hbar}\int_{\tau_2'}^{t} d\tau \overline{W}_e(\mathbf{q}(\tau))} e^{-\frac{i}{\hbar}\int_{t_0}^{\tau_2'} d\tau \overline{W}_g(\mathbf{q}(\tau))} e^{\frac{i}{\hbar}\int_{\tau_3'}^{t} d\tau \overline{W}_{f\mathbf{k}}(\mathbf{q}(\tau))} e^{\frac{i}{\hbar}\int_{\tau_1'}^{\tau_3'} d\tau \overline{W}_e(\mathbf{q}(\tau))} e^{\frac{i}{\hbar}\int_{t_0}^{\tau_1'} d\tau \overline{W}_g(\mathbf{q}(\tau))} e^{i\omega_{f\mathbf{k},e}(t-\tau_3')} e^{i\omega_{e,g}(\tau_2'-\tau_1')} P_g(\Gamma_{t_0})\Big\}. \tag{41}$$

This expression can be readily calculated numerically by simulating classical trajectories, taken from the distribution P_g [see Eq. (40)].

When the laser pulses are short (impulsive), the envelopes $E^{(j)}(t)$ vanish unless $t \simeq \tau^*$ and the nuclei do not have time to evolve during the pulses. This allows one to calculate the time integrals analytically and approximate the dipole matrix elements by their value at the center of the pulse,

$$E^{(2)}(t)V_{f,e}(\mathbf{q}(t)) \simeq E^{(2)}(t)V_{f,e}(\mathbf{q}(\tau_2)). \tag{42}$$

The phases coming from the $\overline{W}_a$ integrals can also be approximated with the help of the reference Hamiltonian. For instance,

$$E^{(2)}(t)E^{(1)}(\tau_2')e^{-\frac{i}{\hbar}\int_{\tau_2'}^{t} d\tau \overline{W}_e(\mathbf{q}(\tau))} \simeq E^{(2)}(t)E^{(1)}(\tau_2')\exp\left\{-\frac{i}{\hbar}[W_e(\mathbf{q}(\tau_2)) - W_{f\mathbf{k}}(\mathbf{q}(\tau_2))](t-\tau_2)\theta(t-\tau_2)\right.$$
$$\left. -\frac{i}{\hbar}[W_e(\mathbf{q}(\tau_1)) - W_g(\mathbf{q}(\tau_1))](\tau_1-\tau_2')\theta(\tau_1-\tau_2')\right\}, \tag{43}$$

which can be easily derived by noting that $\overline{W}_e$ vanishes for $\tau_1 < \tau < \tau_2$, and that, as a result, the contribution must come from the domains $t > \tau_2$ and $\tau_2 < \tau_1$, which are restricted by the narrow pulses.

The remaining $\overline{W}_a$ integrals in Eq. (41) are approximated similarly, and the results are presented in Appendix. This leads to the following expression for the impulsive signal:

$$\tilde{S}_{sc}^{pp}(\varepsilon,t_1) = -\frac{2}{\hbar^4}\sum_{\varepsilon_{\mathbf{k}}=\varepsilon}\int d\Gamma_{t_0}\int dt\int_{t_0}^{t} d\tau_3'\int_{t_0}^{\tau_3'} d\tau_2' d\tau_1' \mathrm{Im}\left\{i^3 E^{(2)}(t)E^{(2)}(\tau_3')E^{(1)}(\tau_2')E^{(1)}(\tau_1')V_{f,e}(\mathbf{q}(\tau_2))V_{e,g}(\mathbf{q}(\tau_1))V_{f,e}^*(\mathbf{q}(\tau_2))\right.$$
$$\times V_{e,g}^*(\mathbf{q}(\tau_1))\exp\left\{-\frac{i}{\hbar}[W_e(\mathbf{q}(\tau_2)) - W_{f\mathbf{k}}(\mathbf{q}(\tau_2))](t-\tau_3') - \frac{i}{\hbar}[W_e(\mathbf{q}(\tau_1)) - W_g(\mathbf{q}(\tau_1))](\tau_1'-\tau_2')\right\}$$
$$\left.\times\ e^{i\omega_{f\mathbf{k},e}(t-\tau_3')}e^{i\omega_{e,g}(\tau_2'-\tau_1')}P_g(\Gamma_{t_0})\right\}. \tag{44}$$

The time integrations in Eq. (44) are analogous to those of the preceding section. The time-integrated signal is, therefore,

$$\tilde{S}_{sc}^{pp}(\varepsilon,t_1)$$
$$\simeq \frac{\rho_f(\varepsilon)}{\hbar^4}\int d\Gamma_{t_0}\left|V_{fe}(\mathbf{q}(\tau_2))\right.$$
$$\times \tilde{E}^{(2)}[\omega_{f\mathbf{k},e} + W_{f\mathbf{k}}(\mathbf{q}(\tau_2))/\hbar - W_e(\mathbf{q}(\tau_2))/\hbar]V_{eg}(\mathbf{q}(\tau_1))$$
$$\left.\times \tilde{E}^{(1)}[\omega_{eq} + W_e(\mathbf{q}(\tau_1))/\hbar - W_g(\mathbf{q}(\tau_1))/\hbar]\right|^2 P_g(\Gamma_{t_0}). \tag{45}$$

Within the classical Condon approximation the signal is determined by the pulse envelope evaluated at the transition energy differences. While both τ_2 and τ_1 appear in Eq. (45), the invariance of the distribution P_g to the unperturbed dynamics means that the signal only depends on the time delay $t_1 = \tau_2 - \tau_1$. The pump-probe technique allows one to explore the nuclear motion by a 2D spectrum, which depends on ε and t_1. By using a series of pump pulses one can calculate signals of higher dimensions.

Batista *et al.* [9] have used a semiclassical method to calculate the photoelectron signal of an I_2^- anion. Their semiclassical method was based on an approximate wavefunction dynamics. In contrast, the present approximation replaces the dynamics of both ket and bra with solutions of classical equations of motion. Furthermore, the assumption of temporally narrow and separated pulses allowed us to perform all time integrals, resulting in Eq. (45). This equation reveals the role of the pulse parameters and bandshape. The expression for the signal given in Ref. [9] involves a Monte Carlo estimation of the integrals and is, therefore, more general.

V. PHOTOELECTRON SIGNALS GENERATED BY QUANTUM OPTICAL FIELDS

The results of the preceding section can be generalized to include a quantum description of the field. Glauber [18] has developed a hierarchy of multipoint correlation functions of the radiation field aimed primarily at photoelectron detection. His celebrated approach had formed the basis for the field of quantum optics and is widely used in photon correlation measurements and for characterizing light sources (e.g., the Hanbury-Brown-Twiss measurement). In Glauber's formalism the field is given and the focus is on the measurement process. Here, we are interested in spectroscopic applications whereby a known field interacts with a system of interest which has its own structure and dynamics. The field gets entangled with the matter and provides a window for viewing the matter. We show that the signals may be recast as products of matter and field multipoint correlation functions.

The Hamiltonian of a molecule interacting with a quantum optical field is

$$\mathcal{H} = \mathcal{H}_0 + \mathcal{H}_F + \mathcal{H}'(t), \tag{46}$$

where

$$\mathcal{H}_F = \sum_s \hbar\omega_s \hat{a}_s^\dagger \hat{a}_s \tag{47}$$

is the radiation field Hamiltonian. $\hat{a}_s^\dagger$ ($\hat{a}_s$) is the creation (annihilation) operator for the s mode of the field. These satisfy the boson commutation rule $[\hat{a}_s^\dagger, \hat{a}_{s'}] = \delta_{ss'}$. The field-matter interaction now takes the form,

$$\mathcal{H}'(t) = -\hat{E}(t)\hat{V} = -[\hat{\mathcal{E}}(t) + \hat{\mathcal{E}}^\dagger(t)]\hat{V}, \tag{48}$$

where $\hat{\mathcal{E}}(t)$ is in the interaction picture with respect to the field Hamiltonian;

$$\hat{\mathcal{E}}(t) \equiv \sum_s \left(\frac{2\pi\hbar\omega_s}{\Omega}\right)^{\frac{1}{2}} \hat{a}_s e^{-i\omega_s t} \tag{49}$$

is the positive frequency part of the field, while Ω is the quantization volume.

We make two simplifying assumptions. The interaction with the field is separated into pump pulses and a detection pulse, so that we can write $\hat{\mathcal{E}} = \hat{\mathcal{E}}^p + \hat{\mathcal{E}}^d$. This separation can be based either on the field frequencies, or on time for well-separated pulses. The unperturbed state of the field should reflect this separation. In addition, we assume that initially the field and matter degrees of freedom are uncorrelated $\hat{\rho}_0 = \hat{\rho}_{0,\text{field}} \otimes \hat{\rho}_{0,\text{matter}}$. This leads to the photoelectron signal:

$$\begin{aligned}\tilde{S}(\varepsilon) = \frac{1}{\hbar^2}\mathrm{Tr}\int_{-\infty}^{t} d\tau_3 \exp_-\left[-\frac{i}{\hbar}\int_{-\infty}^{\tau_3} d\tau_4 \hat{E}^p(\tau_4)\hat{V}(\tau_4)\right] \\ \times \hat{E}^d(\tau_3)\hat{V}(\tau_3)\hat{P}^f(t)\int_{-\infty}^{t} d\tau_1 \hat{E}^d(\tau_1)\hat{V}(\tau_1) \\ \times \exp_+\left[\frac{i}{\hbar}\int_{-\infty}^{\tau_1} d\tau_2 \hat{E}^p(\tau_2)\hat{V}(\tau_2)\right]\hat{\rho}_0(t_0).\end{aligned} \tag{50}$$

The various operators in Eq. (50) are expressed in the interaction picture with respect to the Hamiltonian $\mathcal{H}_0 + \mathcal{H}_F$. Comparison with the previous section highlights one crucial difference between a classical and a quantum description of the field. The projection $\hat{P}^f$ operates only on the material degrees of freedom. The material degrees of freedom can be factorized but the two terms are multiplied by a field correlation function, which depends on all time variables. The signal no longer factorizes into a product of two amplitudes.

As an example, we consider the simplest pump-probe signal, which in the case of classical fields is given by Eq. (27). The ket and the bra interact once with the pump pulse. Expanding both exponentials in Eq. (50) to first order, we find

$$\begin{aligned}\tilde{S}_{pp}(\varepsilon,t_1) = \hbar^{-4}\int_{-\infty}^{t} d\tau_1 d\tau_2 d\tau_3 d\tau_4 \theta(\tau_4-\tau_3)\theta(\tau_1-\tau_2) \\ \times \langle g(t_0)|\hat{V}(\tau_4)\hat{V}(\tau_3)|f(t)\rangle\langle f(t)|\hat{V}(\tau_1)\hat{V}(\tau_2)|g(t_0)\rangle \\ \times \langle \hat{E}^p(\tau_4)\hat{E}^d(\tau_3)\hat{E}^d(\tau_1)\hat{E}^p(\tau_2)\rangle_{\text{field}},\end{aligned} \tag{51}$$

where $\langle\cdots\rangle_{\text{field}}$ denotes the average over the initial density matrix of field degrees of freedom. For a classical field $\langle \hat{E}^p(\tau_4)\hat{E}^d(\tau_3)\hat{E}^d(\tau_1)\hat{E}^p(\tau_2)\rangle_{\text{field}} = E^p(\tau_4)E^d(\tau_3)E^d(\tau_1)E^p(\tau_2)$ and we recover the results of Sec. III. However, Eq. (51) can describe fields with nonclassical correlations.

Equation (51) provides a time-domain representation for the signal. To derive a frequency-domain representation similar to that of Sec. III we substitute the interaction picture field (49) in (50) and perform the time integrals, leaving sums over field modes instead. The calculation is similar to that of Sec. II, except that we now define a transition amplitude which is an operator in the field degrees of freedom:

$$\begin{aligned}\hat{T}_{fg}(t) \equiv \langle f(t)| - \sum_{\substack{s_1\in d\\ p_1=\pm}} \left(\frac{2\pi\hbar\omega_{s_1}}{\Omega}\right)^{\frac{1}{2}} \hat{a}_{s_1}^{p_1} e^{-ip_1\omega_{s_1}t}\hat{V}(t) \\ \times \exp_+\left[\frac{i}{\hbar}\int_{-\infty}^{t} d\tau \sum_{\substack{s_2\in p\\ p_2=\pm}}\left(\frac{2\pi\hbar\omega_{s_2}}{\Omega}\right)^{\frac{1}{2}} \hat{a}_{s_2}^{p_2} e^{-ip_2\omega_{s_2}\tau}\hat{V}(\tau)\right] \\ \times |g(t_0)\rangle e^{\frac{i}{\hbar}\varepsilon_g(t-t_0)}.\end{aligned} \tag{52}$$

In Eq. (52) we have assumed that the pump and detection pulses have different frequencies, leading to the different domains of summation. We have also introduced a compact notation for the positive and negative frequency contributions of the field. For $p_j = +$ one should substitute $p_j\omega_{s_j} = +\omega_{s_j}$ and $\hat{a}_{s_j}^{p_j} = \hat{a}_{s_j}$, while for $p_j = -$ we have $p_j\omega_{s_j} = -\omega_{s_j}$ and $\hat{a}_{s_j}^{p_j} = \hat{a}_{s_j}^\dagger$.

Expanding (52) in powers of the interaction, calculating the time integration, and Fourier transforming leads to

$$\begin{aligned}\hat{T}_{fg}(\omega) = \sum_{\substack{s_1\in d\\ p_1=\pm}} \left(\frac{2\pi\hbar\omega_{s_1}}{\Omega}\right)^{\frac{1}{2}} \hat{a}_{s_1}^{p_1}\tilde{T}_{fg}^{(1)}(p_1\omega_{s_1})2\pi\delta(\omega - p_1\omega_{s_1}) \\ +\hbar^{-1}\sum_{\substack{s_1\in p\\ p_1=\pm}}\sum_{\substack{s_2\in d\\ p_2=\pm}}\left[\prod_{i=1}^{2}\left(\frac{2\pi\hbar\omega_{s_i}}{\Omega}\right)^{\frac{1}{2}}\right]\hat{a}_{s_2}^{p_2}\hat{a}_{s_1}^{p_1}\tilde{T}_{fg}^{(2)}(p_2\omega_{s_2},p_1\omega_{s_1})2\pi\delta(\omega - p_1\omega_{s_1} - p_2\omega_{s_2}) \\ +\hbar^{-2}\sum_{\substack{s_1\in p\\ p_1=\pm}}\sum_{\substack{s_2\in p\\ p_2=\pm}}\sum_{\substack{s_3\in d\\ p_3=\pm}}\left[\prod_{i=1}^{3}\left(\frac{2\pi\hbar\omega_{s_i}}{\Omega}\right)^{\frac{1}{2}}\right]\hat{a}_{s_3}^{p_3}\hat{a}_{s_2}^{p_2}\hat{a}_{s_1}^{p_1}\tilde{T}_{fg}^{(3)}(p_3\omega_{s_3},p_2\omega_{s_2},p_1\omega_{s_1})2\pi\delta(\omega - p_1\omega_{s_1} - p_2\omega_{s_2} - p_3\omega_{s_3}) + \cdots.\end{aligned} \tag{53}$$

Equation (53) extends Eq. (18) to quantum fields. The photoelectron signal, is now given by

$$\tilde{S}(\varepsilon) = \frac{1}{\hbar^2}\rho_f(\varepsilon)\mathrm{tr}\hat{T}_{fg}(\omega_{fg})\hat{\rho}_{0,\mathrm{field}}\hat{T}^{\dagger}_{gf}(\omega_{fg}), \tag{54}$$

where tr denotes the trace over field degrees of freedom. As stated earlier, only the material but not the field degrees of freedom factorize.

The first few terms in the expansion of (54) in matter-field interactions are given by

$$\begin{aligned}\tilde{S}(\varepsilon) = \frac{4\pi^2}{\hbar^2}\rho_f(\varepsilon)\Bigg\{ & \sum_{\substack{s_1,s_2\in d\\ p_1,p_2=\pm}}\left[\prod_{i=1}^{2}\left(\frac{2\pi\hbar\omega_{s_i}}{\Omega}\right)^{\frac{1}{2}}\right]\langle \hat{a}_{s_2}^{-p_2}\hat{a}_{s_1}^{p_1}\rangle_{\mathrm{field}}\tilde{T}^{(1)*}_{fg}(p_2\omega_{s_2})\tilde{T}^{(1)}_{fg}(p_1\omega_{s_1})\delta(\omega_{fg}-p_1\omega_{s_1})\,\delta(\omega_{fg}-p_2\omega_{s_2})\\ & +\frac{1}{\hbar}\sum_{\substack{s_2,s_2\in d;s_1\in p\\ p_1,p_2,p_3=\pm}}\left[\prod_{i=1}^{3}\left(\frac{2\pi\hbar\omega_{s_i}}{\Omega}\right)^{\frac{1}{2}}\right]\Big(\langle \hat{a}_{s_3}^{-p_3}\hat{a}_{s_2}^{p_2}\hat{a}_{s_1}^{p_1}\rangle_{\mathrm{field}}\tilde{T}^{(1)*}_{fg}(p_3\omega_{s_3})\tilde{T}^{(2)}_{fg}(p_2\omega_{s_2},p_1\omega_{s_1})\\ & +\langle \hat{a}_{s_1}^{-p_1}\hat{a}_{s_2}^{-p_2}\hat{a}_{s_3}^{p_3}\rangle_{\mathrm{field}}\tilde{T}^{(2)*}_{fg}(p_2\omega_{s_2},p_1\omega_{s_1})\tilde{T}^{(1)}_{fg}(p_3\omega_{s_3})\Big)\delta(\omega_{fg}-p_3\omega_{s_3})\delta(\omega_{fg}-p_1\omega_{s_1}-p_2\omega_{s_2})+\cdots\Bigg\}.\end{aligned} \tag{55}$$

Equation (55) has the following structure: each term factorizes into a product of two (material) transition amplitudes, multiplied by a single field correlation function. For classical (coherent state) fields the field correlation function also factorizes, and we recover the results of Sec. II. Properties of the field, such as the bandshape, or the time delays between pulses, are encoded in the expectation values appearing in Eq. (55). Multipoint field correlation functions form the basis of Glauber's theory of photon counting [18]. That theory uses normally ordered operator products. The present application requires instead time ordering in a closed-time-path-loop. Normal ordering does not play a role.

The expressions derived here may be used to compute photoelectron signals induced by entangled optical or x-ray photons [24–28]. These should provide many new control parameters that could be explored in the future.

The present expressions involving correlation functions of the fields may also be used to represent stochastic fluctuating classical fields rather than quantum fields. This issue is of interest since many of the intense x-ray sources are noisy. The multipoint correlation functions are, however, different and in that case there is no entanglement with the field. For example, in some applications of the pump-probe technique with entangled photons we have $\langle \hat{E}_1\hat{E}_2\hat{E}_3\hat{E}_4\rangle = \langle \hat{E}_4\hat{E}_3\rangle\langle \hat{E}_2\hat{E}_1\rangle$ and Eq. (51) then can be restored to the form of an amplitude square [31,32]. Such factorizations are not expected for stochastic fields.

VI. ELECTRON VERSUS PHOTON DETECTION

In the pump-probe setup it is also possible to measure directly the absorption of the probe pulse, rather than the photoelectrons. The two signals are expected to be similar, as they result from the same process. However, usually electrons are easier to detect and they contain some complementary information due to the fact that the PES signal depends on the electron kinetic energy, while the photon signal depends on the frequency of the absorbed light. We now compare the two types of signals. PES signals are recast as the modulus square of transition amplitudes, whereas heterodyne detected optical signals are given by nonlinear susceptibilities and can be dissected into material fluxes (which are given by squared amplitudes) and parametric contributions which only involve exchange of photons between the fields and leave the matter intact. Parametric processes do not contribute to 2DPES.

We define the photon signal using a quantum description of the field. We use the total Hamiltonian,

$$\mathcal{H} = \mathcal{H}_0 + \mathcal{H}_F + \mathcal{H}'(t), \tag{56}$$

where

$$\mathcal{H}_F = \sum_s \hbar\omega_s \hat{a}_s^{\dagger}\hat{a}_s \tag{57}$$

is the radiation field Hamiltonian. $\hat{a}_s^{\dagger}$ ($\hat{a}_s$) is the creation (annihilation) operator for the s mode of the field. These bosonic operators satisfy the commutation rule $[\hat{a}_s^{\dagger},\hat{a}_{s'}] = \delta_{ss'}$. The field-matter interaction takes the form,

$$\mathcal{H}'(t) = -\hat{E}(t)\hat{V} = -[\hat{\mathcal{E}}(t)+\hat{\mathcal{E}}^{\dagger}(t)]\hat{V}, \tag{58}$$

where

$$\hat{\mathcal{E}}(t) \equiv \sum_s \left(\frac{2\pi\hbar\omega_s}{\Omega}\right)^{\frac{1}{2}}\hat{a}_s e^{-i\omega_s t} \tag{59}$$

is the positive frequency part of the field, while Ω is the quantization volume.

The photon signal is defined as the change of the occupation number of photons [33],

$$S_{\mathrm{ph}} \equiv \int dt \frac{d}{dt}\langle \hat{\mathcal{N}}\rangle, \tag{60}$$

where

$$\hat{\mathcal{N}} = \sum_s \hat{a}_s^\dagger \hat{a}_s. \tag{61}$$

The signal is calculated using the Heisenberg equation of motion for $\hat{\mathcal{N}}$. The commutator $[\mathcal{H},\hat{\mathcal{N}}]$ is calculated explicitly. We assume that the field is in a coherent state, thereby replacing the field operators $\hat{E}(t)$ by their classical analogous $E(t)$ (neglecting spontaneous emission). The resulting expression for the photon signal is [33]

$$S_{\rm ph} = \frac{2}{\hbar}\int dt \mathrm{Im}\left\langle \mathcal{T}\mathcal{E}(t)\hat{V}_L \exp_+\left[-\frac{i}{\hbar}\int_{-\infty}^{t} d\tau\sqrt{2}\mathcal{H}'_-(\tau)\right]\right\rangle. \tag{62}$$

Equation (62) was obtained by first calculating the rate of transitions, and then integrating over time. The same approach can also be used for the photoelectron signal, and can help to compare the signals. This equivalent expression for the photoelectron signal is derived by explicitly calculating the time derivative of Eq. (5), rearranging the terms, and finally integrating over time. This leads to

$$\tilde{S}(\varepsilon) = \frac{2}{\hbar}\int dt \mathrm{Im}\left\langle \mathcal{T}\hat{P}_L^f(t)\mathcal{H}_L^d(t) \times \exp_+\left[-\frac{i}{\hbar}\int_{-\infty}^{t} d\tau\sqrt{2}\mathcal{H}'_-(\tau)\right]\right\rangle. \tag{63}$$

Comparison of Eq. (62) with Eq. (63) shows that the two signals differ by an overall sign, the projection $\hat{P}^f$, and the appearance of the complex field amplitude $\mathcal{E}(t)$ instead of the full field $E(t)$. The projection $\hat{P}^f$ in Eq. (63) eliminates transitions to nonscattering states. However, we assume that the frequencies in the ionizing pulse are tuned to match the scattering ionized states, and that, as a result, the appearance of $\hat{P}^f$ in Eq. (63) or its absence in Eq. (62) do not lead to any practical difference. Similarly, $\mathcal{E}(t)$ is the positive frequency component of $E(t)$, that is, $\tilde{\mathcal{E}}(\omega) = \tilde{E}(\omega)\theta(\omega)$. By convention, the contributions to the photoelectron signal in, say, Eq. (45) are always evaluated at positive frequencies.

As a result of these considerations, the calculation of the photon absorption of the probe reduces to the one already performed for photoelectrons. It gives

$$\tilde{S}_{\rm ph}^{pp}(t_1) = -\int d\varepsilon \tilde{S}^{pp}(\varepsilon,t_1), \tag{64}$$

where $\tilde{S}^{pp}$ is given by Eq. (27) or Eq. (45). This signal is integrated over the pulse, but still depends parametrically on the delay time between the pump and the probe. The overall negative sign simply reflects our definition of the photon signal (60), since the number of photons decreases for absorption. Equation (64) assumes that the linear absorption during the probe can be neglected, due to energy mismatch. The t_1 independent linear absorption signal can be calculated similarly.

The photoelectron signal (45) depends on the photoelectron kinetic energy. In contrast, the photon signal, Eq. (64), describes the total photon absorption over all the photon frequencies. It is possible to disperse the photon signal, and to measure the absorption at a given probe frequency. This signal is obtained simply by limiting the frequency arguments of $\tilde{\mathcal{E}}^{(2)}$. We find

$$\tilde{S}_{\rm ph}^{pp}(\omega_2,t_1) = -\int d\varepsilon \int d\Gamma_{t_0}\frac{\rho_f(\varepsilon)}{\hbar^4}P_g(\Gamma_{t_0}) \times \left| V_{fe}(\mathbf{q}(\tau_2))\tilde{E}^{(2)}(\omega_2)V_{eg}(\mathbf{q}(\tau_1)) \times \tilde{E}^{(1)}\left(\omega_{eg}+\frac{W_e(\mathbf{q}(\tau_1))-W_g(\mathbf{q}(\tau_1))}{\hbar}\right)\right|^2 \times \delta\left(\omega_2-\omega_{f\mathbf{k},e}-\frac{W_{f\mathbf{k}}(\mathbf{q}(\tau_2))-W_e(\mathbf{q}(\tau_2))}{\hbar}\right). \tag{65}$$

Both Eqs. (65) and (45) correspond to the same process, and are composed of the same building blocks. However, they depend on different energy variables. In Eq. (65) this is the frequency of the probe, and this signal therefore depends on the bandshape $\tilde{\mathcal{E}}^{(2)}(\omega)$. In contrast, the photoelectron kinetic energy is given by $\varepsilon = \hbar\omega_1 + \hbar\omega_2 - \hbar\omega_{fg}$, where ω_j is the frequency absorbed by interacting with the jth pulse. As a result, the photoelectron signal is some kind of convolution of both bandshapes. The photoelectron and the photon absorption signals, therefore, carry similar but complementary information, resulting from their different energy dependence.

VII. CONCLUSIONS

We have derived correlation function expressions for PES signals generated by sequences of short optical or x-ray pulses. The approach is formally similar to nonlinear spectroscopy with photon detection, except that the PES signals can be expressed as transition amplitudes. The present theory may be used to predict the roles of pulse bandshapes and other pulse parameters. PES with quantum fields and entangled photons is another promising future direction.

ACKNOWLEDGMENTS

Support from Chemical Sciences, Geosciences and Biosciences Division, Office of Basic Energy Sciences, Office of Science, US Department of Energy is gratefully acknowledged.

APPENDIX: APPROXIMATE EVALUATION OF INTEGRALS FOR IMPULSIVE PULSES

Applying the short pulse approximation to several factors appearing in Eq. (41), we find,

$$E^{(1)}(\tau_2')e^{-\frac{i}{\hbar}\int_{t_0}^{\tau_2'}d\tau\overline{W}_g} = E^{(1)}(\tau_2')\exp\left\{-\frac{i}{\hbar}[W_g(\mathbf{q}(\tau_1)) - W_e(\mathbf{q}(\tau_1))](\tau_2'-\tau_1)\theta(\tau_2'-\tau_1)\right\}, \tag{A1}$$

$$E^{(1)}(\tau_1')e^{\frac{i}{\hbar}\int_{t_0}^{\tau_1'} d\tau \overline{W}_g} = E^{(1)}(\tau_1')\exp\left\{\frac{i}{\hbar}[W_g(\mathbf{q}(\tau_1)) - W_e(\mathbf{q}(\tau_1))](\tau_1' - \tau_1)\theta(\tau_1' - \tau_1)\right\}, \tag{A2}$$

$$E^{(1)}(\tau_1')E^{(2)}(\tau_3')e^{\frac{i}{\hbar}\int_{\tau_1'}^{\tau_3'} d\tau \overline{W}_e} = E^{(1)}(\tau_1')E^{(2)}(\tau_3')\exp\left\{\frac{i}{\hbar}[W_e(\mathbf{q}(\tau_2)) - W_{f\mathbf{k}}(\mathbf{q}(\tau_2))](\tau_3' - \tau_2)\theta(\tau_3' - \tau_2)\right.$$
$$\left. + \frac{i}{\hbar}[W_e(\mathbf{q}(\tau_1)) - W_g(\mathbf{q}(\tau_1))](\tau_1 - \tau_1')\theta(\tau_1 - \tau_1')\right\}, \tag{A3}$$

and, finally,

$$E^{(2)}(t)E^{(2)}(\tau_3')e^{\frac{i}{\hbar}\int_{\tau_3'}^{t} d\tau \overline{W}_{f\mathbf{k}}} = E^{(2)}(t)E^{(2)}(\tau_3')\exp\left\{\frac{i}{\hbar}[W_{f\mathbf{k}}(\mathbf{q}(\tau_2)) - W_e(\mathbf{q}(\tau_2))](\tau_2 - \tau_3')\theta(\tau_2 - \tau_3')\right.$$
$$\left. - \frac{i}{\hbar}[W_{f\mathbf{k}}(\mathbf{q}(\tau_2)) - W_e(\mathbf{q}(\tau_2))](\tau_2 - t)\theta(\tau_2 - t)\right\}, \tag{A4}$$

which is valid for $t > \tau_3'$.

Equations (43) and (A1)–(A4) combine in such a way that all the step functions are canceled. This results in the rather simple dependence of Eq. (44) on the nuclear potentials W_a.

[1] F. Groot and A. Kotani, *Core Level Spectroscopy of Solids* (CRC Press, Boca Raton, 2008).
[2] J. Stöhr, *NEXAFS Spectroscopy* (Springer-Verlag, Berlin, 1996).
[3] M. Wolf, Surf. Sci. **377**, 343 (1997).
[4] C. A. Schmuttenmaer *et al.*, Phys. Rev. B **50**, 8957 (1994).
[5] S. Xu, J. Cao, C. C. Miller, D. A. Mantell, R. J. D. Miller, and Y. Gao, Phys. Rev. Lett. **76**, 483 (1996).
[6] H. Petek, M. J. Weida, H. Nagano, and S. Ogawa, Science **288**, 1402 (2000).
[7] H. R. Hudock, B. G. Levine, A. L. Thompson, H. Satzger, D. Townsend, N. Gabor, S. Ullrich, A. Stolow, and T. J. Martinez, J. Phys. Chem. A **111**, 8500 (2007).
[8] H. R. Hudock and T. J. Martinez, Chem. Phys. Chem. **9**, 2486 (2008).
[9] V. S. Batista, M. T. Zanni, J. Greenblatt, D. M. Neumark, and W. H. Miller, J. Chem. Phys. **110**, 3736 (1999).
[10] N.-H. Ge, C. M. Wong, and C. B. Harris, Acc. Chem. Res. **33**, 111 (2000).
[11] M. Drescher *et al.*, Science **291**, 1923 (2001); F. Krausz and M. Ivanov, Rev. Mod. Phys. **81**, 163 (2009).
[12] M. M. Murnane, H. C. Kapteyn, M. D. Rosen, and R. W. Falcone, Science **251**, 531 (1991); W. Li *et al.*, *ibid.* **322**, 1207 (2008).
[13] LCLS: The first experiments.
[14] P. H. Bucksbaum, Science **317**, 766 (2007).
[15] M. F. Kling and M. J. J. Vrakking, Annu. Rev. Phys. Chem. **59**, 463 (2008).
[16] R. Ernst, G. Bodenhausen, and A. Wokaun, *Principles of Nuclear Magnetic Resonance in One and Two Dimensions* (Clanderon Press, Oxford, 1998).
[17] S. Mukamel *et al.*, Acc. Chem. Res. **42**, 553 (2009).
[18] R. Glauber, *Quantum Theory of Optical Coherence: Selected Papers and Lectures* (Wiley-VCH, New York, 2007).
[19] S. Rahav and S. Mukamel, Proc. Natl. Acad. Sci. USA. **107**, 4825 (2010).
[20] S. Mukamel and S. Rahav, Adv. At. Mol. Opt. Phys. **59** (to be published).
[21] R. Weinkauf, P. Schanen, D. Yang, S. Soukara, and E. W. Schlag, J. Phys. Chem. **99**, 11255 (1995); R. Weinkauf *et al.*, *ibid.* **100**, 18567 (1996).
[22] F. Remacle and R. D. Levine, Proc. Natl. Acad. Sci. USA. **103**, 6793 (2006).
[23] R. Santra, N. V. Kryzhevoi, and L. S. Cederbaum, Phys. Rev. Lett. **103**, 013002 (2009).
[24] O. Roslyak, C. A. Marx, and S. Mukamel, Phys. Rev. A **79**, 033832 (2009).
[25] B. E. A. Saleh, B. M. Jost, H. B. Fei, and M. C. Teich, Phys. Rev. Lett. **80**, 3483 (1998).
[26] B. Dayan, A. Pe'er, A. A. Friesem, and Y. Silberberg, Phys. Rev. Lett. **93**, 023005 (2004).
[27] H. Kimble and S. van Enk, Nature **429**, 712 (2004).
[28] D. Lee and T. Goodson, J. Phys. Chem. B **110**, 25582 (2006).
[29] U. Harbola and S. Mukamel, Phys. Rep. **465**, 191 (2008).
[30] A. E. Cohen and S. Mukamel, Phys. Rev. Lett. **91**, 233202 (2003).
[31] O. Roslyak and S. Mukamel, Phys. Rev. A **79**, 063409 (2009).
[32] A. Muthukrishnan, G. S. Agarwal, and M. O. Scully, Phys. Rev. Lett. **93**, 093002 (2004).
[33] C. A. Marx, U. Harbola, and S. Mukamel, Phys. Rev. A **77**, 022110 (2008).
[34] J. Zyss and I. Ledoux, Chem. Rev. **94**, 77 (1994).
[35] I. V. Schweigert and S. Mukamel, Phys. Rev. A **77**, 033802 (2008).
[36] R. Bernstein and A. H. Zewail, J. Chem. Phys. **90**, 829 (1989).
[37] L. E. Fried and S. Mukamel, J. Chem. Phys. **93**, 3063 (1990).
[38] S. Mukamel, *Principles of Nonlinear Optical Spectroscopy* (Oxford University Press, Oxford, 1995).